Spectroscopy of new CH_3OH FIR laser lines pumped by new CO_2 laser lines

LI-HONG XU[1] AND R.M. LEES[2]
Centres of Excellence in Molecular and Interfacial Dynamics (CEMAID) and Physics Department, University of New Brunswick, Fredericton, NB E3B 5A3, Canada

K.M. EVENSON
Time and Frequency Division, National Institute of Standards and Technology, Boulder, CO 80303, U.S.A.

C.-C. CHOU AND J.-T. SHY
Physics Department, National Tsing Hua University, Hsinchu, Taiwan 30043, Republic of China

AND

E.C.C. VASCONCELLOS
Instituto de Física, Departamento de Eletrônica Quântica UNICAMP, 13.081 Campinas SP, Brazil

Received April 7, 1994
Accepted May 19, 1994

This paper is dedicated to Dr. Gerhard Herzberg on the occasion of his 90th birthday

The number of CO_2 laser lines available for optical pumping of far-infrared (FIR) lasers has been significantly increased by the development of a new continuous wave (cw) CO_2 laser at the Time and Frequency Division of the National Institute of Standards and Technology in Boulder, Colorado. This system operates on very high-J lines of the normal bands as well as on sequence and new hot-band lines, and has generated numerous new FIR laser transitions in CH_3OH. These include the new 123 μm world-record holder, pumped by the 9HP(20) hot-band CO_2 line, which is now the most efficient known FIR laser line. Assignments are given for a number of the IR pump – FIR laser energy level and transition systems, based on our high-resolution Fourier transform studies of the FIR and IR spectra of CH_3OH. Features of the transition system for the 123 μm line and wave numbers for several further potential FIR laser lines are presented.

La division des Temps et Fréquences de l'Institut National des Standards et de la Technologie de Boulder au Colorado a récemment développé un nouveau laser cw CO_2 qui augmente de façon significative le nombre de lignes laser disponibles pour le pompage optique de lasers dans l'IR lointain (FIR). Il opère dans les lignes de J élevé de la bande normale ainsi que dans des bandes de séquence et de nouvelles « bandes chaudes ». Il permet d'induire un grand nombre de transitions FIR dans le CH_3OH, incluant la nouvelle « championne du monde » à 123 μm, optenue par ligne 9HP(20) de la « bande chaude » du CO_2. Elle est reconnue comme la plus efficace bande laser FIR connue à ce jour. Nous présentons le résultat de nos études sur les lasers FIR. Nous identifiions quelques niveaux et transitions pour un laser FIR pompé à l'IR sur la base d'un calcul à haute résolution de transformées de Fourier des spectres FIR et IR de CH_3OH. Nous ajoutons quelques remarques sur les transitions du système produisant la ligne à 123 μm et proposons, avec une précision de ±0,001 cm^{-1}, quelques autres lignes candidates pour un système laser FIR.

[Traduit par la rédaction]

Can. J. Phys. 72, 1155 (1994)

1. Introduction

The present paper discusses the optical pumping of CH_3OH with an improved CO_2 laser [1] at the Time and Frequency Division of the National Institute of Standards and Technology in Boulder to obtain far-infrared (FIR) laser emission with new CO_2 pumping lines. Our spectroscopic data on the infrared (IR) and FIR absorption spectra of CH_3OH have been applied to the assignment of several of the new IR pump – FIR laser energy level and transition systems. One system of particular interest involves a very strong FIR laser line at 123 μm, and we consider some aspects of the system that contribute to the high efficiency for this line.

Methanol is arguably the most important lasing medium for the generation of FIR laser radiation by optical pumping with a CO_2 laser, and more than 570 lines have been reported so far for the normal CH_3OH isotopic species [2]. This extensive emission arises because of the good overlap between methanol IR absorption and the CO_2 laser bands. The methanol IR absorption spectrum is so rich that almost every CO_2 laser line, from the $9R(34)$ to $9P(46)$ and $10R(48)$ to $10P(32)$ transitions as well as sequence band and isotopic CO_2 laser lines [2], is able to hit a molecular absorption and produce FIR laser radiation. Recently, a particularly efficient new CO_2 laser was developed at the Time and Frequency Division of the National Institute of Standards and Technology in Boulder that operates not only on very high-J lines of the normal bands and on sequence band lines, but also on more than 40 hot-band lines with a power of up to 8 W [1, 3]. This new source has significantly enhanced the possibilities for new laser lines; in fact, 27 new FIR laser lines have been observed for 11 different pump lines. Among these, the 123 μm FIR laser line is now the most efficient known, more than twice as powerful as the well-known previous record holder at 119 μm [4].

The identification of the specific molecular transitions giving rise to the observed FIR laser emission is an interesting spectroscopic challenge, because these transitions generally lie within the torsion-rotation energy level manifold of an excited vibrational state and therefore are not observable by normal absorption spectroscopy. However, it is possible to extract the excited state energy pattern indirectly through the use of IR and

[1] Present address: Molecular Physics Division, National Institute of Standards and Technology, Gaithersburg, MD 20899, U.S.A.
[2] Author to whom correspondence may be addressed.

Printed in Canada / Imprimé au Canada

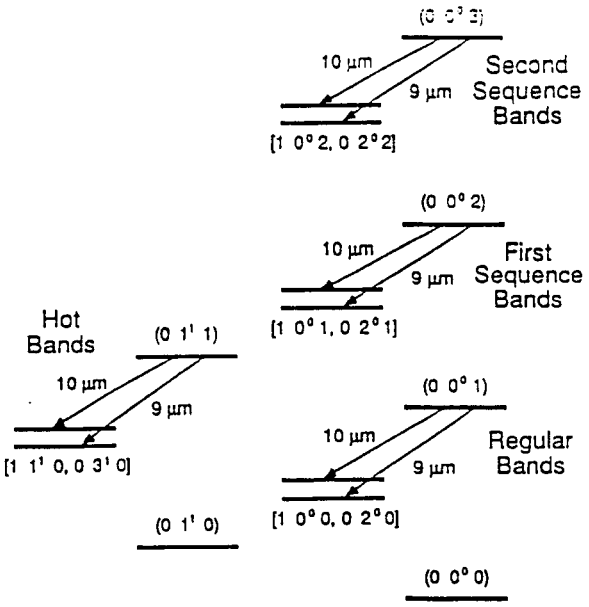

FIG. 1. Vibrational energy level diagram for CO_2, showing the various laser bands. The level (v_1 v_2^l v_3) quantum numbers denote the symmetric stretching (v_1), degenerate bending (v_2^l) and asymmetric stretching (v_3) modes.

FIR spectroscopy by forming combination differences in the combination-loop technique. We construct a closed loop of transitions, with the FIR laser line forming the top, two IR absorptions from ground to excited state forming the sides, and a ground-state FIR absorption closing the loop at the bottom. Since the IR and FIR sides of the loop can be measured to high accuracy by high-resolution Fourier transform spectroscopy, the wave number of the remaining FIR laser side of the loop is determined to a similar accuracy. This procedure gives reliable and unambiguous results and has been employed to determine or to confirm the assignments of a large number of FIR laser lines for CH_3OH [5] and several other isotopic variants of methanol [6–8].

The success of methanol as a laser-active medium is due principally to the good overlap between the CO-stretching band in methanol and the CO_2 laser bands, although increasing numbers of FIR laser lines have been assigned to other vibrational states such as the CH_3-rocking and CH_3-deformation modes. High-resolution spectroscopy of the CO-stretching band of methanol dates from 1978 with the early diode laser study by Sattler et al. [9, 10], but received great impetus in the 1980s from the commercial development of Fourier transform spectrometers for the IR and FIR regions. The first high-resolution Fourier transform spectrum of the CO-stretching band of CH_3OH was in fact recorded by J.W.C. Johns at the Herzberg Institute of Astrophysics in Ottawa in 1982 to initiate a collaboration between our group and G. Moruzzi and F. Strumia of the University of Pisa. Since then, there has been much study and collaborative work on both this IR band and the FIR torsion-rotation spectrum in the ground state [11–17], so that our present knowledge of the ground-state and CO-stretch energy level manifolds of CH_3OH is quite extensive.

Since the first observation of optically pumped FIR laser radiation from CH_3OH in 1970 [18], the understanding of the spectroscopy and of the FIR laser emission have more or less proceeded hand-in-hand. The first major breakthrough in identifying the FIR laser transitions came in 1977 with assignment papers by Henningsen [19] and Danielewicz and Coleman [20], about the same time as the initial high-resolution spectral studies. Since then, there has been steady progress in extending the assignments of both the spectra and the FIR laser lines, with considerable cross-fertilization between the two problems. The use of the combination loops for the FIR laser identification checks not only the assignment of the laser lines but also of the other IR and FIR transitions in the loops and has provided very valuable confirmations of the spectroscopic work.

The FIR laser emission has turned out, in a remarkably large number of cases, to be a sensitive indicator of perturbations in the spectrum and has revealed important interactions among different vibrational states. A notable example involved clever detective work by Henningsen, who was first able to assign a large and puzzling group of FIR laser lines to a consistent energy level scheme involving a mysterious "X-state" interacting strongly with the CO-stretch [21] and later went on to demonstrate that this was actually the CH_3-rocking mode in strong Coriolis resonance with the CO-stretch [22]. Another important insight by Weber and Maker for CD_3OH [23] was the realization that strong Fermi resonances would occur due to level-crossings in which highly excited torsional levels of the ground state cross the CO-stretching state at a sharp angle and produce substantial shifts and mixing at very specific locations in the energy level diagram. They noted that these Fermi resonances would exist for all isotopic species and for other vibrational states as well, and numerous instances have since been observed, many of which have led to FIR lasing [7, 8].

Thus, while the push to assign the specific transitions associated with reported FIR laser lines might not appear at first glance to lead directly to fundamental progress in determining molecular constants, this work has in fact been a driving force behind a significant number of important discoveries made in recent years about vibrational resonances and interactions in methanol. These have substantially increased our knowledge of the excited states and point the way toward better understanding of the molecular potential and the anharmonic coupling terms [24, 25]. Furthermore, the impetus from the investigation of the FIR emission has led to the acquisition of rich and extensive high-resolution IR and FIR Fourier transform spectra which are now available as excellent reference spectra for test or calibration purposes, and are already coming into use for the perennially difficult task of accurate calibration of diode laser spectra [26, 27].

2. Features of the new Boulder CO_2 laser

The success of the newly developed CO_2 laser is associated with the use of high-resolution specially blazed gratings and a ribbed laser discharge tube [1, 3], both of which improve the mode structure and lead to a high effective resolution in the laser cavity. The higher resolution permits weaker lines to lase that are otherwise in competition with the regular lines, and also leads to a considerable extension of the customary operating range of the laser. As the grating is rotated, the laser is scanned through its output lines, and with the appropriate choice of grating can be made to oscillate on all the regular lines from $R(62)$ to $P(62)$ including $R(0)$, on many of the 10.8 μm hot-band lines, on many of the 10 μm sequence band lines, on some of the 9 μm sequence lines, and on a substantial number of the lines of the new 9 μm hot band. The identification of the 9 μm hot-band lines was originally confirmed by close agreement between direct

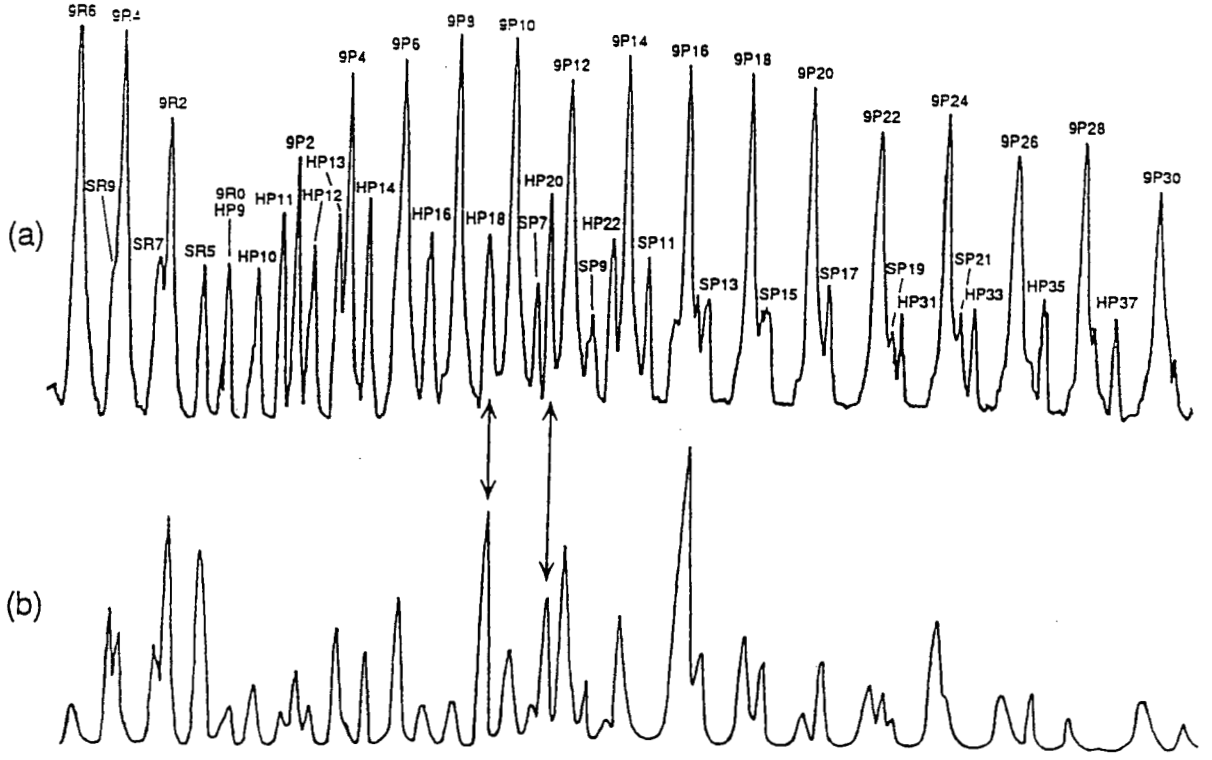

FIG. 2. (*a*) Scan of the CO_2 laser in the 9.4 μm band showing regular, hot-band (H) and sequence-band (S) lines; (*b*) CH_3OH optoacoustic signals observed for the CO_2 laser scan. The arrows indicate the positions of the 9HP(18) and 9HP(20) hot-band lines; the latter pumps the very efficient 123 μm FIR laser line.

heterodyne measurements of the frequencies of the HP(42) and HP(43) members of the band and the values calculated from the best available molecular constants [1]. The frequencies of all of the new high-J regular lines plus the 9 μm and 10 μm hot-band lines have now been measured by heterodyning with a second fluorescence-stabilized CO_2 laser and the results used in a least-squares fit to improve the molecular constants and yield more precise frequencies for the $^{12}C^{16}O_2$, $^{13}C^{16}O_2$, $^{12}C^{18}O_2$, and $^{13}C^{18}O_2$ isotopomers [3].

The CO_2 vibrational energy diagram is shown in Fig. 1, illustrating the regular, sequence, and hot-band transitions, with the (v_1 v_2^l v_3) quantum numbers of a vibrational level denoting the symmetric stretching (v_1), degenerate bending (v_2^l), and asymmetric stretching (v_3) modes. The upper levels of the regular and sequence bands are the successive excited states of the asymmetric-stretching mode. These are in near degeneracy with the successive N_2 vibrationally excited states, leading to the population of the upper lasing levels by resonant energy exchange. The lower lasing levels are the mixed [1 $0^0 v_3$, 0 2^0 v_3] doublets formed from Fermi resonance between the symmetric-stretch fundamental and second excited bending states, with successive quanta of the asymmetric stretch added in. The hot-band levels differ from those of the regular bands in having one additional quantum of bend and are the (0 1^1 1) → [1 1^1 0, 0 3^1 0] transitions.

In Fig. 2*a*, we illustrate a scan of the new CO_2 laser over part of its operating profile. The initial lines of the regular 9*R* band including *R*(0) are seen to the left, then part of the 9*P* band on the right. Between the lines of the strong regular bands, transitions of the sequence band and the new 9 μm hot band are clearly visible, showing the wealth of lines available with this laser for optical pumping. The excellent potential for production of new FIR laser emission with this laser is seen in Fig. 2*b*, which shows the signal observed by passing the CO_2 beam through an optoacoustic cell containing 133 Pa of CH_3OH. The numerous resonances indicate coincidences with CH_3OH IR absorptions for almost all of the CO_2 laser lines in all three of the laser bands. Particularly strong optoacoustic signals are observed for the 9HP(18) and 9HP(20) hot-band lines as highlighted by the arrows in Fig. 2, pointing to good chances for significant FIR laser output by pumping with those transitions.

3. New FIR laser lines optically pumped by the Boulder CO_2 laser

As suggested from the optoacoustic observations, FIR laser emission is indeed seen with the new pumping lines, and so far 27 new FIR laser lines have been observed in 11 different transition systems pumped by 8 of the 9 μm hot-band CO_2 laser lines and 3 of the sequence-band lines. The observations are given in Table 1, which lists the pumping lines, their frequencies and wave numbers, and all of the new FIR laser wavelengths and wave numbers. The hot-band and sequence-band pumping lines are denoted by H and S. In practice, the FIR laser emission was very sensitive to the operating conditions, particularly the CH_3OH pressure employed and the precise orientation of the antenna pattern of the MIM diode detector; hence, considerable care was needed to explore all conditions as fully as possible to try to ensure that all laser lines had been observed. To detect selectively the lines in specific FIR wavelength regions, we placed quartz and paper filters of different thicknesses in the FIR

TABLE 1. New CH_3OH FIR laser lines optically pumped by hot-band (H) and sequence-band (S) lines of the Boulder CO_2 laser

CO_2 pump line	CO_2 Pump frequency (MHz)	CO_2 Pump wave number[a] (cm^{-1})	FIR Laser wavelength (μm)	FIR Laser wave number (cm^{-1})
9HP(43)	30 948 763.097	1032.339 62	108.6	92.08
			154.1	64.89
9HP(20)	31 614 686.312	1054.552 42	123.4515	81.003 46[b]
			170.4645	58.663 24[b]
			447.9406	22.324 39[b]
9HP(18)	31 669 349.252	1056.375 78	157.6	63.45
			224.3	44.58
			302.9	33.01
			464.4	21.53
9HP(16)	31 723 189.941	1058.171 72	90.0	111
			120.7	82.85
9HP(14)	31 776 250.508	1059.941 63	85.2	117
			108.8	91.91
9HP(13)	31 804 759.363	1060.892 58	111.6	89.61
			272.3	36.72
9HP(09)	31 906 376.996	1064.282 18	71.1	141
9HR(23)	32 629 513.084	1088.403 40	123.1	81.23
			165.7	60.35
9SR(5)	31 927 605.052	1064.990 27	120.0	83.33
			229.0	43.67
			286.0	34.97
9SR(7)	31 970 979.208	1066.437 08	84.3	119
9SR(9)	32 013 527.621	1067.856 34	63.3	158
			118.6	84.32
			209.8	47.66
			274.5	36.43
			392.4	25.48

[a] Converted from frequency, using the factor 1 cm^{-1} = 29 979.2458 MHz.
[b] Determined from accurate heterodyne frequency measurement. Fractional uncertainty is $\pm 2 \times 10^{-7}$.

beam in front of the detector to isolate particular ranges of wave number.

The FIR wavelengths were determined by scanning a Fabry–Perot interferometer through a series of fringes, as illustrated in Fig. 3 for the 9HP(16) pump. Two different FIR laser lines are present simultaneously, as revealed on the trace by sequences of peaks with different periodicities. However, Fig. 3 also shows that the line of longer wavelength is oscillating in two different modes since two trains of peaks, denoted as a and a' are visible in the scan instead of just one. The uniform spacing of the a and a' peak trains reveals them to have identical wavelengths and thus to correspond to a single FIR line. Similarly, there is an additional mode b' visible for line b towards the right side of Fig. 3, but with greatly reduced intensity. From the Fabry–Perot scans, the FIR laser wavelengths were determined within about ± 0.5 μm, representing a fairly large uncertainty in wave number. Thus, the use of our Fourier transform data to achieve an uncertainty of about ± 0.001 cm^{-1} for predicted FIR laser wave numbers from combination differences constitutes a significant improvement in precision.

4. Fourier transform spectra and notation

The IR and FIR spectroscopic results employed in this work to identify the FIR laser transitions came from several sources. Our Fourier transform spectrum of the strong CO-stretching band centred around 1033 cm^{-1} was recorded in 1988 from 930 to 1100 cm^{-1} at 0.002 cm^{-1} resolution on the spectrometer at the Herzberg Institute of Astrophysics. Several studies of this band have been reported in the past, and the structure is well characterized [9–13, 28–30]. For the FIR torsion-rotation band in the ground vibrational state, transition wave numbers above 80 cm^{-1} were derived from our analysis of a Fourier transform spectrum recorded at 0.004 cm^{-1} resolution, also on the National Research Council instrument in Ottawa. Below 80 cm^{-1}, we employed the results obtained through our collaboration with the Pisa group [14–17], utilizing FIR spectra recorded at better than 0.002 cm^{-1} resolution on B. Carli's spectrometer at the University of Florence and that of M. and B.P. Winnewisser at Justus-Liebig University in Giessen. A few of the assignments and wave numbers in the original reports were revised in the later work; hence, below 80 cm^{-1} we took the current up-to-date data from the FIR line atlas on computer diskette available from G. Moruzzi [16].

In general, the measurement uncertainties for both the IR and FIR spectra are estimated to be ± 0.0005 cm^{-1} for unblended lines, so the wave numbers of the transitions going around a closed four-sided loop should sum to 0 to within about ± 0.001 cm^{-1} if all the transition assignments are correct. This condition, applied to as many independent closed combination loops as possible, was the principal test that we used to determine and to check our FIR laser assignments. The specific transition wave numbers used in the loops are collected in Table 2 for reference, with the IR transitions labelled with capital letters, $\Delta K = \pm 1$ b-type FIR transitions labelled with lower-case letters, and $\Delta K = 0$ a-type transitions labelled with Greek letters. In this work, we followed the Dennison convention common in the FIR

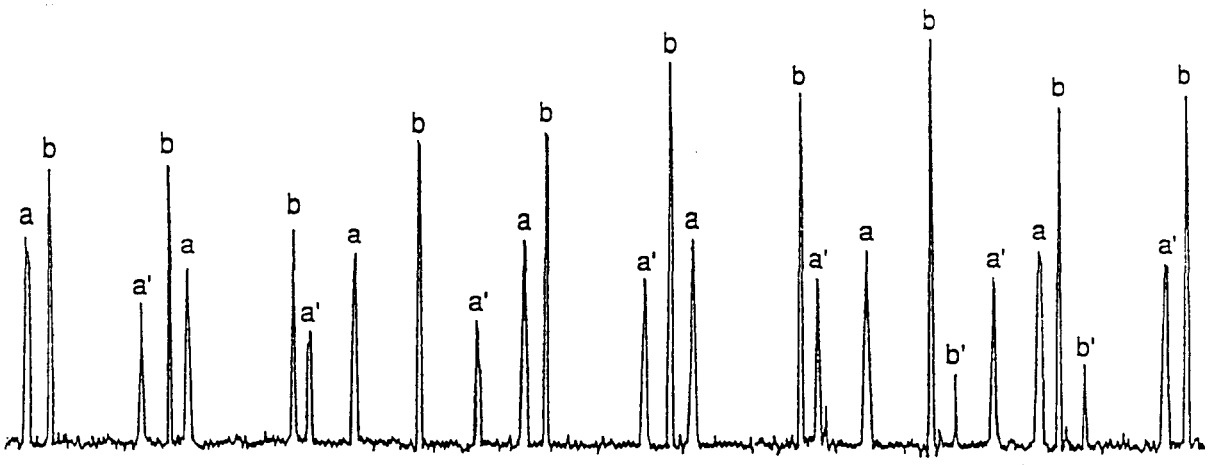

FIG. 3. Fabry–Perot scan showing the 120.7 and 90.0 μm FIR laser lines (*a* and *b*, respectively) optically pumped by the 9HP(16) hot-band CO_2 laser line. Peak trains *a* and *a'* , and *b* and *b'*, correspond to pairs of different cavity modes for the same FIR laser line.

laser literature of labelling an energy level as $(n\tau K,J)^{v}$. In this notation, n is the quantum number for the torsional state, τ is an index equal to 1, 2, or 3 that defines the torsional A, E_1, or E_2 symmetry species according to the rule $(\tau + K)\text{mod}3 = 0$, 1, or 2 for E_1, A, and E_2, respectively [31], K is the projection of the rotational angular momentum J along the molecular a-axis, and v indicates the vibrational state. We denote the ground vibrational state as v = o, the CO stretch as v = co, and the in-plane CH_3-rocking mode as v = r.

5. Assignments of the new FIR laser lines

In our investigation of the new FIR laser observations, we have so far determined firm spectroscopic assignments for 10 of the lines and tentative identifications for 2 others. The assignments and other relevant details are collected in Table 3 for each of the IR pump – FIR laser systems and are discussed below.

5.1. IR pump transitions

Column 2 of Table 3 lists the CO_2 laser pump lines and wave numbers ν_L for the different systems. The assignments of the CH_3OH parent IR-pump absorptions coincident with these pump lines are presented in column 3, along with the observed wave numbers ν_{IR} from our Ottawa Fourier transform spectrum. The pump offsets $(\nu_{IR} - \nu_L)$ are given in column 4, as calculated from the differences between the observed IR and the known CO_2 laser pump wave numbers.

5.2. FIR laser transitions

Column 5 specifies the transition routes for the observed and predicted FIR laser lines associated with each IR pump. The FIR laser assignments proposed here primarily involve $n = 0$ levels of the first excited CO-stretching state, with the exception of systems 3 and 5. In system 5, the transitions are among torsionally excited levels of the CO-stretching state, while in system 3 the pumping is to the upper u component of the hybridized $[(025,14)^{co}/(034,14)^{r}]$ doublet in the excited vibrational state, as shown in Fig. 4. This hybridization is the result of Coriolis mixing between the near-degenerate $(025)^{co}$ levels of the CO-stretching state and $(034)^{r}$ levels of the in-plane methyl-rocking state [21, 22]. For J =14, the upper component of the hybrid doublet is the one with greater rocking-state character; hence the stronger FIR lines expected are in effect $(034)^{r} \rightarrow (013)^{r}$ rocking-state transitions, shown as L_d and L_e in Fig. 4.

5.3. Polarization

The FIR laser emission will be linearly polarized either parallel or orthogonal to the pump depending on the J-value changes in the pump and FIR laser transitions, denoted by ΔJ_{pump} and ΔJ_{FIR}. The relative polarization for each FIR laser line is shown in column 8, and is given by the rules:

$$\Delta J_{pump} + \Delta J_{FIR} = \text{even} \Rightarrow \parallel$$

$$\Delta J_{pump} + \Delta J_{FIR} = \text{odd} \Rightarrow \perp$$

These rules can thus point to the J-numbering of the FIR laser lines and are important clues to the assignments. However, in this work, the polarizations were not measured for most of the lines, but were only predicted from the spectroscopic analysis.

5.4. FIR laser wave numbers

The observed FIR laser wave numbers ν_{obs} are given in column 7 of Table 3. For systems 1–4, the three FIR laser lines L_a, L_b, and L_c should follow the so-called triad rule with $L_a \approx (L_c - L_b)$, as seen for system 2. This rule arises because both L_a and $(L_c - L_b)$ correspond to $\Delta K = 0$ a-type transitions, which are relatively insensitive to the $(n\tau K)$ quantum numbers. The rule is useful in identifying the a-type laser line L_a and thereby determining the J'-value of the upper pumped level as $J' \approx L_a/2B'$, where B' is the rotational B-value for the upper state. Most of the ν_{obs} values are derived from the measured wavelengths; we have estimated their uncertainties to be a few tenths of one inverse centimetre. Those for system 2 were obtained from precise heterodyne FIR laser frequency measurements with a fractional uncertainty of $\pm 2 \times 10^{-7}$.

For each of the systems, we could employ our high-resolution spectroscopic data to calculate the majority of the FIR laser wave numbers from combination differences to an uncertainty of ± 0.001 cm^{-1}. The resulting ν_{calc} wave numbers and examples of the specific combination relations used are given in columns 9 and 10 of Table 3. The combination-loop approach to wave number prediction is demonstrated more fully in the next section for the new 123 μm line, at present the world's most efficient known FIR laser line. Several of the systems still have potential FIR laser lines that might be observed in future; loop-calculated

TABLE 2. Transition wave numbers (in cm^{-1}) for the FIR laser systems of CH_3OH

	CO stretch IR transitions[a]			Ground state FIR transitions			
System	Label	$P/Q/R(n\tau K, J)$	ν_{obs}[b]	Label	$(n'\tau'K', J')$ ←	$(n''\tau''K'', J'')$	ν_{obs}[b,c]
1	*P*	$Q(0211,17)^{co}$	1032.3403*	*a*	$(0211,17)^o$ ←	$(0310,16)^o$	91.9859
	A	$R(0211,16)^{co}$	1059.6947*	*b*	$(0211,16)^o$ ←	$(0310,15)^o$	90.3901
	B	$R(0211,15)^{co}$	1058.391*	*c*	$(0211,16)^o$ ←	$(0310,16)^o$	64.6312
	C	$P(0211,17)^{co}$	1005.2868*	*d*	$(0211,15)^o$ ←	$(0310,15)^o$	64.6403
	D	$R(0310,16)^{co}$	1059.0987				
	E	$R(0310,15)^{co}$	1057.7433*				
2	*P*	$R(018,13)^{co}$	1054.5527	*a*	$(018,15)^o$ ←	$(027,14)^o$	83.4305
	A	$R(018,12)^{co}$	1053.1771	*b*	$(018,14)^o$ ←	$(027,13)^o$	81.8259
	B	$P(018,14)^{co}$	1009.6711	*c*	$(018,13)^o$ ←	$(027,12)^o$	80.2204
	C	$P(018,15)^{co}$	1007.8300*	*d*	$(018,15)^o$ ←	$(027,15)^o$	59.2606
	D	$P(027,15)^{co}$	1008.4273	*e*	$(018,14)^o$ ←	$(027,14)^o$	59.2645*
	E	$P(027,14)^{co}$	1010.2570	*f*	$(018,13)^o$ ←	$(027,13)^o$	59.2686
	F	$R(027,13)^{co}$	1055.1582	*g*	$(018,12)^o$ ←	$(027,12)^o$	59.2719
	G	$R(027,12)^{co}$	1053.7697	*h*	$(018,14)^o$ ←	$(027,15)^o$	35.0948
				i	$(018,13)^o$ ←	$(027,14)^o$	36.7074*
				j	$(018,12)^o$ ←	$(027,13)^o$	38.3197
3	*P*	$R(025^u,13)^h$	1056.3764	*a*	$(025,15)^o$ ←	$(034,14)^o$	64.1523
	A	$R(025^u,12)^h$	1054.8285*	*b*	$(025,14)^o$ ←	$(034,13)^o$	62.5500*
	B	$P(025^u,14)^h$	1011.3003	*c*	$(025,13)^o$ ←	$(034,12)^o$	60.9459*
	C	$P(025^u,15)^h$	1009.6286	α	$(025,15)^o$ ←	$(025,14)^o$	24.1794
	D	$P(034,15)^{co}$	1008.3280	β	$(025,14)^o$ ←	$(025,13)^o$	22.5694
	E	$P(034,14)^{co}$	1010.1969	γ	$(025,13)^o$ ←	$(025,12)^o$	20.9584
	F	$R(034,13)^{co}$	1055.0920	*d*	$(034,15)^o$ ←	$(013,14)^o$	45.4122†
	G	$R(034,12)^{co}$	1053.7382	*e*	$(034,14)^o$ ←	$(013,13)^o$	43.7999†*
				f	$(034,13)^o$ ←	$(013,12)^o$	42.1882†
				δ	$(034,15)^o$ ←	$(034,14)^o$	24.1865
				ε	$(034,14)^o$ ←	$(034,13)^o$	22.5757
				φ	$(034,13)^o$ ←	$(034,12)^o$	20.9641
4	*P*	$R(017,21)^{co}$	1064.9921	*a*	$(017,23)^o$ ←	$(026,22)^o$	86.4190
	A	$R(017,20)^{co}$	1063.7530	*b*	$(017,22)^o$ ←	$(026,21)^o$	84.8346*
	B	$P(017,23)^{co}$	992.5789*	*c*	$(017,21)^o$ ←	$(026,20)^o$	83.2454
	C	$P(017,22)^{co}$	994.5435	*d*	$(017,23)^o$ ←	$(026,23)^o$	49.3929
	D	$R(026,21)^{co}$	1066.0229*	*e*	$(017,22)^o$ ←	$(026,22)^o$	49.4110*
	E	$R(026,20)^{co}$	1064.6864	*f*	$(017,21)^o$ ←	$(026,21)^o$	49.4277*
	F	$P(026,23)^{co}$	993.5735	*g*	$(017,20)^o$ ←	$(026,20)^o$	49.4422
	G	$P(026,22)^{co}$	995.4462				
5	*P*	$R(212,22)^{co}$	1067.8553*	*a*	$(212,24)^o$ ←	$(133,25)^o$	78.1648
	A	$R(212,21)^{co}$	1066.7086	*b*	$(212,23)^o$ ←	$(133,24)^o$	79.6050
	B	$P(212,24)^{co}$	992.4540	*c*	$(212,22)^o$ ←	$(133,23)^o$	81.0645
	C	$P(212,23)^{co}$	994.5035	*d*	$(212,21)^o$ ←	$(133,22)^o$	82.5387
	D	$R(133,23)^{co}$	1064.3807	*e*	$(212,24)^o$ ←	$(133,24)^o$	118.1057
	E	$R(133,22)^{co}$	1063.1621	*f*	$(212,23)^o$ ←	$(133,23)^o$	117.9663
	F	$P(133,25)^{co}$	986.0800	*g*	$(212,22)^o$ ←	$(133,22)^o$	117.8419
	G	$P(133,24)^{co}$	988.0249				

[a] The $(025^u, J)^h$ transitions are to the upper *u* components of hybridized $[(025, J)^{co}/(034, J)^r]$ doublets mixed by Coriolis resonance.
[b] Lines marked with asterisks are overlapped, and have uncertain accuracy.
[c] Wave numbers with daggers are the mean values for close asymmetry doublets.

redictions for the wave numbers of these transitions are ıcluded in Table 3.

The proposed assignments of the rocking-state laser lines L_d nd L_e in the 9HP(18) system 3 illustrated in Fig. 4 should still e regarded as tentative, since IR spectroscopic data are not vailable for the methyl-rocking band of CH_3OH so that combination loops could not be formed. Therefore, the approximate wave numbers given in Table 3 for the rocking-state laser lines were derived from energy levels calculated with estimated constants, notably a torsional barrier height V_3 of 557 cm^{-1} [32]. Although the qualitative agreement with the observations is persuasive, the calculation did not take the

TABLE 3. Assignments of new FIR laser lines in CH_3OH optically pumped by the Boulder CO_2 laser

System	CO_2 pump (ν_L in cm^{-1})	IR absorption[a] (ν_{IR} in cm^{-1})	Offset (MHz)	FIR laser transition[b] $(n'\tau'K',J')^{v'} \rightarrow (v''\tau''K'',J'')$	Line label	ν_{obs} (cm^{-1})	Rel Pol	ν_{calc}[b] (cm^{-1})	Loop relation[c]
1	9HP(43)	Q(0211,17)	20	$(0211,17)^{co} \rightarrow [(0211,16)^{co}]$	$[L_a]$		[⊥]	[27.0535]	$P-C$
	1032.339 62	1032.3403		$\rightarrow (0310,17)^{co}$	L_b	64.89	[∥]	65.2275	$P+a-D$
				$\rightarrow (0310,16)^{co}$	L_c	92.08	[⊥]	92.3415	$A+b-E$
2	9HP(20)	R(018,13)	9	$(018,14)^{co} \rightarrow (018,13)^{co}$	L_a	22.32439[c]	[∥]	22.3245	$P+f-j-A$
	1054.552 42	1054.5527		$\rightarrow (027,14)^{co}$	L_b	58.66324[c]	⊥	58.6631	$P+f-F$
				$\rightarrow (027,13)^{co}$	L_c	81.00346[c]	∥	81.0034	$P+c-G$
				$[(027,14)^{co}] \rightarrow [(027,13)^{co}]$	$[L_d]$		[∥]	[22.3402]	$D-d+a-E$
3	9HP(18)	$R(025^u,13)^h$	18	$(025^u,14)^h \rightarrow [(025^u,13)^h]$	$[L_a]$		[∥]	[22.5067]	$P-\beta-B$
	1056.375 78	1056.3764		$\rightarrow [(034,14)^{co}]$	$[L_b]$		[⊥]	[41.2662]	$P+c-\phi-F$
				$\rightarrow (034,13)^{co}$	L_c	63.45	[∥]	63.5841	$P+c-G$
				$\rightarrow (013,14)^r$	L_d	21.53	[⊥]	22.6[d]	
				$\rightarrow (013,13)^r$	L_e	44.58	[∥]	45.1[d]	
4	9SR(5)	R(017,21)	55	$(017,22)^{co} \rightarrow (017,21)^{co}$	L_a	34.97	[∥]	35.0423	$P+c-g-A$
	1064.990 27	1064.9921		$\rightarrow (026,22)^{co}$	L_b		[⊥]	[48.3983]	$B+d-F$
				$\rightarrow (026,21)^{co}$	L_c	83.33	[∥]	83.5511	$P+c-E$
5	9SR(9)	R(212,22)	−31	$(212,23)^{co} \rightarrow (212,22)^{co}$	L_a	36.43	[∥]	36.4500	$P+c-f-C$
	1067.856 34	1067.8553		$\rightarrow [(133,23)^{co}]$	$[L_b]$		[⊥]	[122.5351]	$P+g-E$
				$\rightarrow (133,24)^{co}$	L_c	84.32	[∥]	84.5388	$B+a-F$

[a] $(025^u, J)^h$ levels are the upper components of Coriolis-mixed hybridized $[(025, J)^{co}/(034, J)^r]$ doublets.
[b] Transitions and relative polarizations in brackets are predicted.
[c] Converted from accurate heterodyne frequency measurements, with 1 cm^{-1} = 29 979.2458 MHz.
[d] Calculated assuming a torsional barrier height of 557 cm^{-1} for the in-plane CH_3-rocking mode.
[e] Transition labels and wave numbers are given in Table 2.

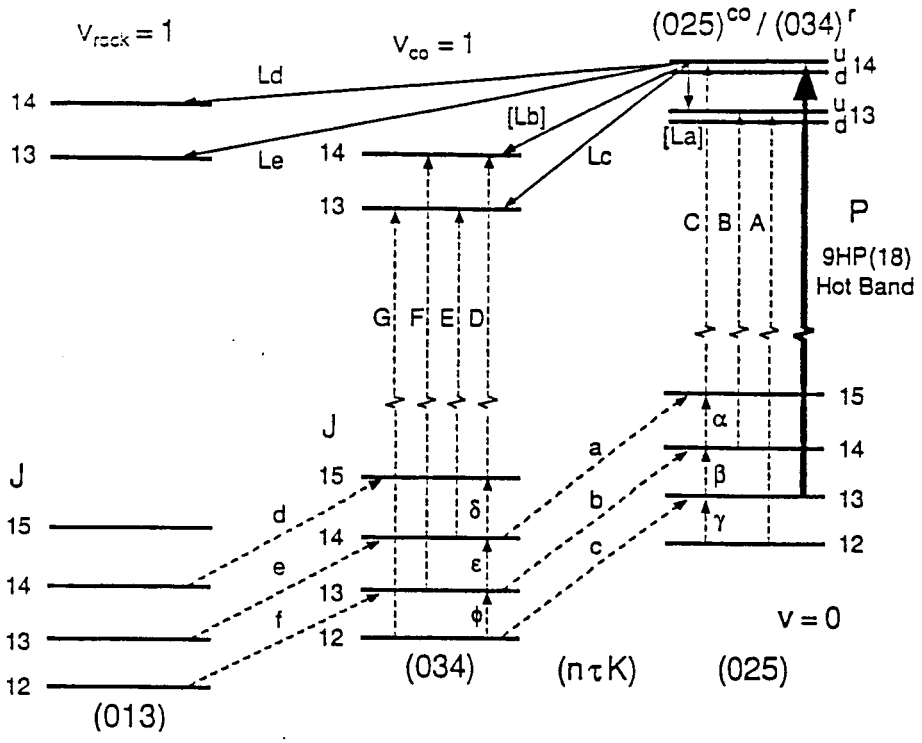

FIG. 4. Energy level and transition diagram proposed for CH_3OH IR pump FIR laser system 3 pumped by the 9HP(18) hot-band CO_2 laser line. The $[(025)^{co}/(034)^{r}]$ u and d levels are upper and lower components of hybridized doublets arising from strong Coriolis mixing between the $(025)^{co}$ and $(034)^{r}$ states. Transition wave numbers are listed in Tables 2 and 3.

Coriolis perturbation into account; hence the accuracies of the predicted wave numbers are uncertain. To test this assignment, which is important in reliably locating the positions of the CH_3-rocking levels, it would be valuable to carry out heterodyne frequency measurements of laser lines L_d and L_e to see if each is in fact a close pair of K-doublet transitions. The $K = 3$ A levels exhibit asymmetry doubling that is clearly resolved in the ground state FIR spectrum, and transitions d, e, and f in Fig. 4 are actually doublets with splittings of 0.0077, 0.0047, and 0.0030 cm^{-1}, respectively [15]. The wave numbers given in Table 2 for these transitions are the mean values for the doublets. While the $K = 3$ doubling will be different in the excited rocking state due to changes in the energy structure with the increased torsional barrier, laser lines L_d and L_e should nevertheless show splittings of a similar order of magnitude that would be readily detectable in a heterodyne measurement. This would provide a stringent test of the assignments.

The 63.45 cm^{-1} laser line L_c for the CO-stretch portion of system 3 in Fig. 4 is well determined from the data of Table 2 through the following combination loops:

$$L_c = P + c - G = 63.5841 \text{ cm}^{-1}$$

$$= C + a - E = 63.5840 \text{ cm}^{-1}$$

The mean loop-calculated wave number of 63.5841 cm^{-1} for line L_c is close to the observed value of 63.45 cm^{-1}, supporting the assignment, while the good agreement between the independent combination loops demonstrates that the spectroscopic assignments are self-consistent. The self-consistency is further evidenced by the loops used to predict the other potential members $[L_a]$ and $[L_b]$ of the FIR laser triad for that system, as follows:

$$[L_a] = P - \beta - B = 22.5067$$

$$= P + \gamma - A = 22.5063$$

$$= C + \alpha - B = 22.5077$$

$$[L_b] = P + c - \phi - F = 41.2662$$

$$= C + a - \delta - D = 41.2664$$

$$= C + \alpha + b - F = 41.2660$$

Further confirmation for the assignment comes from the fact that the $9P(12)$ line of the regular CO_2 band is known to pump the complementary system involving the $R(025^{d},13)^{h}$ IR absorption, and the corresponding laser lines from the lower d level of the $J = 14$ hybrid doublet to the $(034,14)^{co}$ and $(034,13)^{co}$ levels have been observed [2]. The reported loop-calculated wave numbers for these d level partners to our lines $[L_b]$ and L_c are 61.1343 and 38.8159 cm^{-1}, respectively [2], so two independent values for the $J = 14$ $(u - d)$ doublet splitting are obtained directly by subtracting them from our calculated laser wave numbers in Table 3 to give 2.4498 and 2.4503 cm^{-1}. The excellent agreement between these values strongly supports the assignments. Subtraction of the 2.45 cm^{-1} splitting from our L_d and L_e wave numbers in Table 1 gives predicted wave numbers of 19.08 and 42.13 cm^{-1} for the corresponding rocking-state transitions that would occur from the d doublet level. However, the $J = 14$ d level is the component with greater CO-stretch character, and FIR laser emission to the rocking state at these wave numbers has not been reported [2].

System 5 is valuable in confirming earlier assignments by our group of the weak torsionally excited $(n\tau K) = (212)$ and (133) IR subbands of the C–O stretch [30]. Loop-combination relations from the data in Table 2 are well satisfied, and leave no

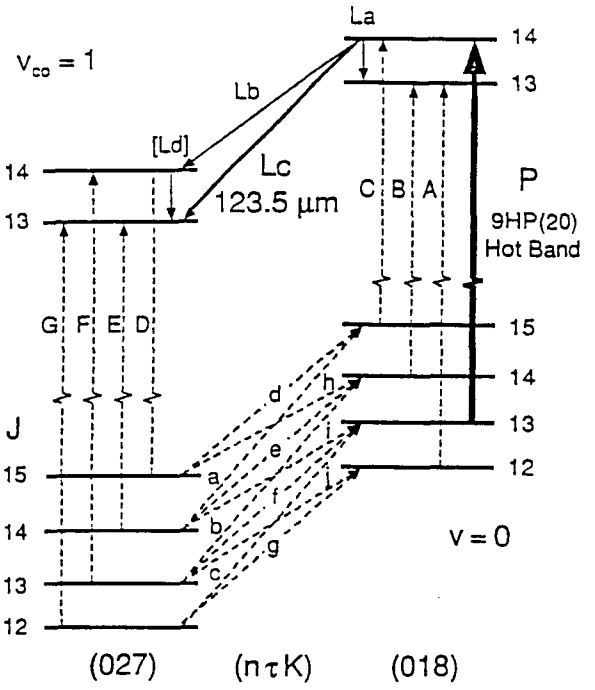

FIG. 5. Transition scheme for system 2 containing the strong 123 μm FIR laser line of CH_3OH pumped by the 9HP(20) hot-band CO_2 line. Transition wave numbers are listed in Tables 2 and 3.

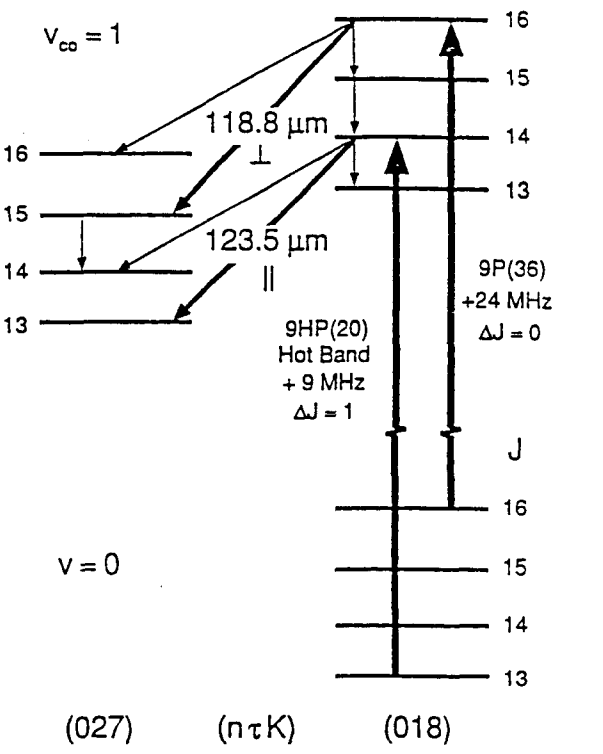

FIG. 6. Comparison of the transition schemes for the new 123 μm line of CH_3OH, presently the most efficient known FIR laser line, and the previous 119 μm record holder.

doubt about the system identification. However, 3 FIR laser lines still remain unaccounted for with the 9SR(9) pump. As this CO_2 line lies in the heart of the region expected for the in-plane CH_3-rocking mode, we might enter the realm of speculation and propose that the 25.48 cm^{-1} FIR laser line is an *a*-type transition pumped by a $Q(16)'$ IR absorption. With an *a*-type wave number being given by $\nu_a \approx 2B'J$, we find for $J = 16$ that $B' = 0.796\ cm^{-1}$, consistent with the typical rotational *B*-values that we calculate for the rocking mode in an excited torsional state. It would be useful here to know the relative polarizations of the unidentified FIR laser lines in this system to look for possible triad relationships and to seek further FIR laser observations to complete the pattern.

6. The IR pump–FIR laser transition system for the 123 μm FIR laser line

The most important system pumped so far by the new CO_2 laser is system 2, with the transition scheme shown in Fig. 5. In this system, the $R(018,13)^{co}$ IR transition is pumped by the 9HP(20) CO_2 hot-band line to give the triad of FIR laser lines at 123.5, 170.5, and 447.9 μm within the excited CO-stretching state. The 123.5 μm line is the most efficient yet observed, approximately twice as strong as the previous 119 μm record holder under similar conditions.

With our high-resolution Fourier transform data, the assignment for this system was rapidly deduced and could be rigorously verified by forming closed combination loops. The calculated wave numbers for lines L_a, L_b, and L_c and the cascade line $[L_d]$ are given from the data in Table 2 as follows:

$$L_a = P + f - j - A = 22.3245$$

$$= C + d - h - B = 22.3247$$

$$L_b = P + f - F = 58.6631$$

$$= C + d - D = 58.6633$$

$$L_c = P + c - G = 81.0034$$

$$= P + i - E = 81.0031$$

$$= C + a - E = 81.0035$$

$$L_d = D - d + a - E = 22.3402$$

$$= D - h + e - E = 22.3400$$

$$= F - f + c - G = 22.3403$$

The frequency of each of the laser lines in this system has been accurately measured, giving wave numbers of $L_a = 22.324\ 39$, $L_b = 58.663\ 24$, and $L_c = 81.003\ 46\ cm^{-1}$. The loop self-consistency and the excellent agreement with these observations leave no doubt about the assignments and confirm that the 123.5 μm line L_c is the $(018,14)^{co} \rightarrow (027,13)^{co}$ transition. In connection with the reliability of the loop calculations, the loop prediction was done for this line before the actual heterodyne frequency measurement was made, and our predicted frequency turned out to be only 1 MHz away from the true value measured subsequently.

This assignment reveals why the new 123 μm line is very strong, because it lies in exactly the same energy level system [4, 5] as the previous 119 μm record holder, but has a smaller pump offset and a higher population in the lower pumped level. The transition scheme for the two lines is given in Fig. 6. The pump offset determined from our spectroscopic data for the

123 μm line is 9 MHz, substantially smaller than that of 24 MHz for the 119 μm line and contributing to the greater efficiency of the 123 μm line. A further advantage for the 123 μm line system is the lower energy of the ground state pump level. This gives a larger Boltzmann factor, which, after account is also taken of the differing $(2J+1)$ spatial M-degeneracies, results in a higher population for pumping by about 15%. Another difference between the systems is the relative polarizations of the pump and FIR laser lines. The 119 μm line is pumped by a $\Delta J = 0$ Q-branch IR absorption while the 123 μm line is pumped by a $\Delta J = 1$ R-branch line. Since both the 119 and 123 μm lines are $\Delta J = 1$ transitions, our polarization rules from Sect. 5.3 imply that the relative polarizations of IR pump and FIR laser line will be perpendicular for the 119 μm line, but parallel for the 123 μm line. This could result in a significant difference in FIR laser output if the FIR cavity is strongly polarization dependent. In the present study, however, both CO_2 pump polarizations were investigated and the optimum was used to determine the efficiency improvement of over a factor of two for the 123 μm line compared to the 119 μm line.

7. Conclusions

In this work, a new efficient CO_2 laser was used for the optical pumping of FIR laser lines in CH_3OH vapour. The CO_2 laser operates on previously unreported lines of the 9 μm hot band, and 8 new FIR laser systems have been observed pumped by these hot-band lines. As well, 3 further FIR laser systems are observed with pumping by sequence-band CO_2 lines. We employed high-resolution Fourier transform spectroscopic data to assign the IR pump and FIR laser transitions for 3 of the hot-band systems and 2 of the sequence-band systems. The assignments are supported by rigorous closed-loop combination difference relations for all of the systems, but are still tentative for part of one system involving transitions to the in-plane CH_3-rocking state for which we have no IR data as yet. The combination loops have permitted prediction of the wave numbers of several further potential FIR laser lines to the Fourier transform uncertainty of ± 0.001 cm^{-1}.

The 123 μm FIR laser line pumped by the 9HP(20) hot-band CO_2 line has the distinction of being the most efficient yet observed; the ratio of FIR output to pump power is more than double that of the 119 μm line. The CO_2 polarization was rotated in this measurement to optimize the polarization for each of the lines. We have found that both lines belong to the same energy level system, involving pumping to excited $(n\tau K) = (018)^{co}$ levels. A somewhat larger population for the ground-state pumped level contributes about 15% to the higher efficiency of the 123 μm line over the 119 μm transition.

Acknowledgements

The research of the University of New Brunswick group was made possible in part by a grant to the Centres of Excellence in Molecular and Interfacial Dynamics (CEMAID), funded by the Networks of Centres of Excellence Programme in association with the Natural Sciences and Engineering Research Council of Canada (NSERC), and by operating support from NSERC and the University of New Brunswick Research Fund. We thank G. Moruzzi for providing a data diskette of the CH_3OH FIR spectrum. L.-H. X. expresses her appreciation to Dr. Evenson for the warm hospitality shown during her visit to the Boulder National Institute of Standards and Technology (NIST) laboratory. It is a great pleasure to acknowledge the major contribution to this research provided through gracious hospitality and Fourier transform spectra from J.W.C. Johns of the Herzberg Institute of Astrophysics, and to acknowledge Gerhard Herzberg himself for friendship, stimulation, leadership, and encouragement for so many years.

1. K.M. Evenson, C.-C. Chou, B.W. Bach, and K.G. Bach. IEEE J. Quantum Electron. **30**, 1187 (1994).
2. G. Moruzzi, J.C.S. Moraes, and F. Strumia. Int. J. Infrared Millimeter Waves, **13**, 1269 (1992).
3. A.G. Maki, C.-C. Chou, K.M. Evenson, L. Zink, and J.-T. Shy. J. Mol. Spectrosc. **167**, 211 (1994).
4. N. Ioli, A. Moretti, and F. Strumia. Appl. Phys. B, **48**, 305 (1989).
5. G. Moruzzi, F. Strumia, R.M. Lees, and I. Mukhopadhyay. Infrared Phys. **32**, 334 (1991).
6. I. Mukhopadhyay, R.M. Lees, W. Lewis-Bevan, J.W.C. Johns, F. Strumia, and G. Moruzzi. Int. J. Infrared Millimeter Waves, **8**, 1483 (1987).
7. I. Mukhopadhyay, M. Mollabashi, R.M. Lees, and J.W.C. Johns. J. Mol. Spectrosc. **138**, 521 (1989).
8. L.-H. Xu, R.M. Lees, I. Mukhopadhyay, and J.W.C. Johns. J. Mol. Spectrosc. **153**, 181 (1992).
9. J.P. Sattler, T.L. Worchesky, and W.A. Riessler. Infrared Phys. **18**, 521 (1978).
10. J.P. Sattler, W.A. Riessler, and T.L. Worchesky. Infrared Phys. **19**, 217 (1979).
11. G. Moruzzi and F. Strumia. Infrared Phys. **24**, 257 (1984).
12. G. Moruzzi, F. Strumia, and F. Colao. Infrared Phys. **25**, 251 (1985).
13. G. Moruzzi, F. Strumia, P. Carnesecchi, R.M. Lees, I. Mukhopadhyay, and J.W.C. Johns. Infrared Phys. **29**, 583 (1989).
14. G. Moruzzi, F. Strumia, C. Bonetti, B. Carli, F. Mencaraglia, M. Carlotti, G. Di Lonardo, and A. Trombetti. J. Mol. Spectrosc. **105**, 24 (1984).
15. G. Moruzzi, F. Strumia, P. Carnesecchi, B. Carli, and M. Carlotti. Infrared Phys. **29**, 47 (1989).
16. G. Moruzzi, P. Riminucci, F. Strumia, B. Carli, M. Carlotti, R.M. Lees, I. Mukhopadhyay, J.W.C. Johns, B.P. Winnewisser, and M. Winnewisser. J. Mol. Spectrosc. **144**, 139 (1990).
17. G. Moruzzi, F. Strumia, J.C.S. Moraes, R.M. Lees, I. Mukhopadhyay, J.W.C. Johns, B.P. Winnewisser, and M. Winnewisser. J. Mol. Spectrosc. **153**, 511 (1992).
18. T.Y. Chang, T.J. Bridges, and E.G. Burkhardt. Appl. Phys. Lett. **17**, 249 (1970).
19. J.O. Henningsen. IEEE J. Quantum Electron. QE-13, 435 (1977).
20. E.J. Danielewicz and P.D. Coleman. IEEE J. Quantum Electron. QE-13, 485 (1977).
21. J.O. Henningsen. J. Mol. Spectrosc. **83**, 70 (1980).
22. J.O. Henningsen. J. Mol. Spectrosc. **91**, 430 (1982).
23. W.H. Weber and P.D. Maker. J. Mol. Spectrosc. **93**, 131 (1982).
24. H. Rudolph, J. Avery, and J.O. Henningsen. J. Mol. Spectrosc. **117**, 38 (1986).
25. L.-H. Xu and R.M. Lees. J. Opt. Soc. Am. B: Opt. Phys. **11**, 155 (1994).
26. P.B. Davies, G.M. Hansford, and T.C. Killian. J. Mol. Spectrosc. **163**, 138 (1994).
27. L.-H. Xu, R.M. Lees, and G. Moruzzi. J. Mol. Spectrosc. **166**, 338 (1994).
28. D.R. Woods. Ph.D. Thesis, University of Michigan, Ann Arbor, Mich., U.S.A. 1970.
29. J.O. Henningsen. J. Mol. Spectrosc. **102**, 399 (1983).
30. I. Mukhopadhyay. Ph.D. Thesis, University of New Brunswick, Fredericton, N.B., Canada. 1986.
31. R.M. Lees and J.G. Baker. J. Chem. Phys. **48**, 5299 (1968).
32. R.M. Lees. J. Chem. Phys. **57**, 824 (1972).